

BRIEF COMMUNICATION

Hydrothermal Synthesis and Characterization of a Novel Mixed-Valence Oxide, $H_xV_2Zr_2O_9 \cdot H_2O$, $x = 0.43$

Guangsheng Pang, Shouhua Feng,¹ Zhongmin Gao, Yaohua Xu, Chunyan Zhao, and Ruren Xu

Key Laboratory of Inorganic Hydrothermal Synthesis and Department of Chemistry, Jilin University, Changchun 130023, People's Republic of China

Received April 16, 1996; in revised form October 16, 1996; accepted October 24, 1996

A novel complex oxide with V(IV, V) mixed valence, $H_xV_2Zr_2O_9 \cdot H_2O$, has been hydrothermally synthesized in a V_2O_5 – ZrO_2 – H_2O system at 240°C for 5 days; NaF was used as a mineralizer. The product crystallizes in a monoclinic system with cell parameters $a = 0.940(4)$ nm, $b = 1.156(8)$ nm, $c = 0.636(3)$ nm, $\beta = 104.1(7)^\circ$, and $V = 0.671(2)$ nm³. The vanadium in the product appears in mixed valence IV and V, which was evidenced by electron paramagnetic resonance analysis. Thermogravimetric analysis showed that the product dehydrated and underwent phase transformations in air and N₂ in the temperature range 500 ~ 600°C. © 1997 Academic Press

thermal crystallization has advantages in making vanadium phosphate compounds with V atoms in mixed IV and V valence, whereas in solid state reactions vanadium phosphates with III and/or V valence are usually formed. With the aim of synthesizing novel complex oxides of double transition metals and on the basis of hydrothermal study on metal phosphates, we begin to study a novel hydrothermal synthesis in V_2O_5 – ZrO_2 – H_2O system. To our knowledge, the formation of double transition metal oxides in hydrothermal systems has not been well studied. Here we report on the hydrothermal synthesis and structural characterization of a novel mixed-valence complex oxide, $H_xV_2Zr_2O_9 \cdot H_2O$, $x = 0.43$.

INTRODUCTION

Recently, the synthesis of a number of vanadium-containing compounds has been extensively studied, since these compounds usually possess particular catalytic and magnetic properties (1–5). The properties and the various novel structures of vanadium compounds are to some degree dependent on the variety of valence states of vanadium; different valent vanadium atoms may adopt different chemical circumstances and lead to different structures. In most vanadium phosphates, the phosphorus atom appears in a PO₄ tetrahedron, while vanadium–oxygen polyhedral building blocks have the ability to adapt various coordination geometries such as significantly distorted octahedra, square pyramids, trigonal bipyramids, and tetrahedra (6). In the vanadium phosphate system, a series of new compounds have been synthesized by both solid state reactions and hydrothermal methods (7–17). Hydrothermal synthesis has been an open route to microporous crystals and metastable phases, and recently this method has been extended to the preparation of novel and nanocrystalline complex oxides and complex fluorides (18–20). We also noted that hydro-

EXPERIMENTAL

The reactants used in the synthesis were NaVO₃·2H₂O (A.R.), NH₄VO₃ (A.R.), ZrOCl₂·8H₂O (A.R.) and NaF (A.R.). The mole composition of the initial reaction mixture was 0.5 V₂O₅:1.0 ZrO₂:1.0 NaF:500 H₂O. A typical synthesis procedure was as follows: 0.525 g NaVO₃·2H₂O, 1.074 g ZrOCl₂·8H₂O, and 0.140 g NaF were mixed in 30 ml H₂O and stirred to make a reaction mixture. The hydrothermal reaction of the reaction mixture was carried in polytetrafluoroethylene lined stainless steel vessels. The reaction proceeded at 240°C under autogenous pressure for 5 days. Brown crystalline product powders were obtained. The product was filtered, washed with deionized water, and dried in air at ambient temperature. The contents of V and Zr in the product were determined with an ICP-AE spectrometer after the sample was fused in Li₂CO₃·HBO₃ and then dissolved in HCl aqueous solution. The contents of components were V, 23.96 wt%; Zr, 40.01 wt%, corresponding to the formula $H_xV_2Zr_2O_9 \cdot H_2O$, $x = 0.43$, in combination with the thermogravimetric (TG), infrared (IR), and electron paramagnetic resonance analyses (EPR).

The powder X-ray diffraction (XRD) analysis was performed on a Rigaku D/max-γA diffractometer with

¹ To whom correspondence should be addressed.

graphite-filtered $\text{CuK}\alpha$ radiation. The adjustment of the diffractometer was checked by using silicon as external standard and the absolute zero error was evaluated at less than 0.01° (2θ). Generator operating conditions were 50 kV and 150 mA, Slit: DS/SS 1° , RS/RS_m 0.15/0.6 mm. Data were collected over the range 10° – 70° with a step interval of 0.02° and a preset time of 4 s per step. The experiment was performed at room temperature. The precise determination of the peak positions, multiplex, and $K\alpha_2$ stripping were carried out by using a program available in the software package of line shape Fourier analysis. The indexing of X-ray powder diffraction patterns and determination of cell parameters of the product were performed by utilizing a locally adapted version of computer program DICVOL91, which is based on the successive dichotomy method and tackles any symmetry (21). The product was indexed in a monoclinic system with cell parameters $a = 0.940(4)$ nm, $b = 1.156(8)$ nm, $c = 0.636(3)$ nm, $\beta = 104.1(7)^\circ$, and $V = 0.671(2)$ nm³ ($M(20) = 23.3$, $F(20) = 36.4(0.0087, 63)$) (22).

The morphology of the crystalline product was observed by scanning electron microscopy (SEM) with a Hitachi X-650 B electron microscope. TG and differential thermal analysis (DTA) were carried out by using Perkin-Elmer DTA-7000, TGA-7 PC series thermal analysis instrument in N_2 or air with a heating rate of $10^\circ\text{C}/\text{min}$. EPR spectra were recorded at room temperature by using BRUKER ER 200D-SRC electron paramagnetic resonance instrument at frequency 9.778 GHz and power 2.05 mW. The field modulation intensity was 1.25 G_{pp}, time constant 500 ms, scan range 2000 G, and mid range 3481 G.

RESULTS AND DISCUSSION

In the hydrothermal synthesis of $\text{H}_x\text{V}_2\text{Zr}_2\text{O}_9 \cdot \text{H}_2\text{O}$, NaVO_3 and NH_4VO_3 can be employed as vanadium sources and when V_2O_5 was used both the product and impurities were obtained. The ratio of V/Zr in the initial reaction mixture affected the formation of the product; when the ratio was in the range 0.5–1.5, keeping pH ca 1–5, pure product can be made. The addition of the mineralizer NaF gave a short reaction time and uniform product particles. The x value can be adjusted from 0.43 to 1.18 by introducing some reduction agents such as HCl and NaI, in this study the x value was 0.43.

Figure 1 shows the EPR spectra of (a) the synthetic product $\text{H}_x\text{V}_2\text{Zr}_2\text{O}_9 \cdot \text{H}_2\text{O}$, (b) the sample after the product was heated in air at 650°C for 1 h, and (c) the sample after the product was heated in N_2 at 650°C for 1 h. It was found from Fig. 1a that the EPR spectrum of vanadium(IV) atoms in the product displayed axial symmetry with $g_\perp = 1.99$, $a_\perp = 7.1$ mT, $g_\parallel = 1.94$, $a_\parallel = 19.4$ mT. From the fine splitting peaks (e.g., no dipole interaction), it can be seen there are a small fraction of vanadium(IV) atoms in the product and from the g and a values it was confirmed that the

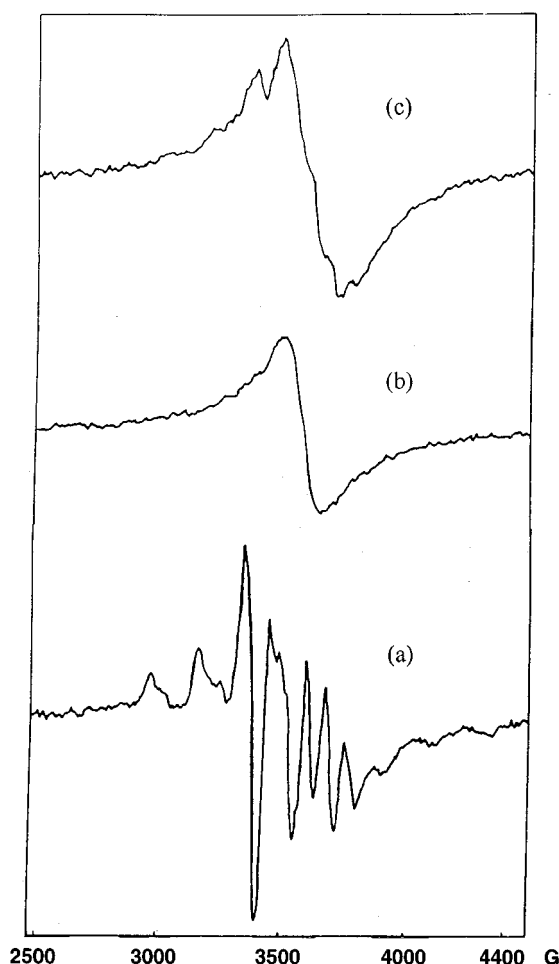


FIG. 1. EPR spectra of (a) $\text{H}_x\text{V}_2\text{Zr}_2\text{O}_9 \cdot \text{H}_2\text{O}$, (b) the sample treated in air at 650°C for 1 h, and (c) the sample treated in N_2 at 650°C for 1 h.

V(IV) atoms are located in an octahedral coordinate environment.

Figure 2 shows the XRD patterns of the products (a) and samples treated at 650°C in air (b) and in N_2 (c). Table 1 lists the powder XRD data of the $\text{H}_x\text{V}_2\text{Zr}_2\text{O}_9 \cdot \text{H}_2\text{O}$ and the indexing results. All diffraction were well indexed in a monoclinic system. The X-ray diffraction pattern of $\text{H}_x\text{V}_2\text{Zr}_2\text{O}_9 \cdot \text{H}_2\text{O}$ is different from those of products treated at 650°C in air and N_2 . This indicates that the structure of the product changes at higher temperature. We also found by XRD that the structure of the sample treated in N_2 is different from that of the sample treated in air. XRD analysis showed that the structure of $\text{H}_x\text{V}_2\text{Zr}_2\text{O}_9 \cdot \text{H}_2\text{O}$ was destroyed after treated at 650°C in air or N_2 for 1 h. Thus, the EPR spectra of the samples treated at 650°C both in air or N_2 are different from that of the product, and there are no well-resolved superfine splitting, demonstrating the existence of adjacent vanadium(V) atoms, but the EPR spectrum of the sample (c) in N_2 showed that there still exist small

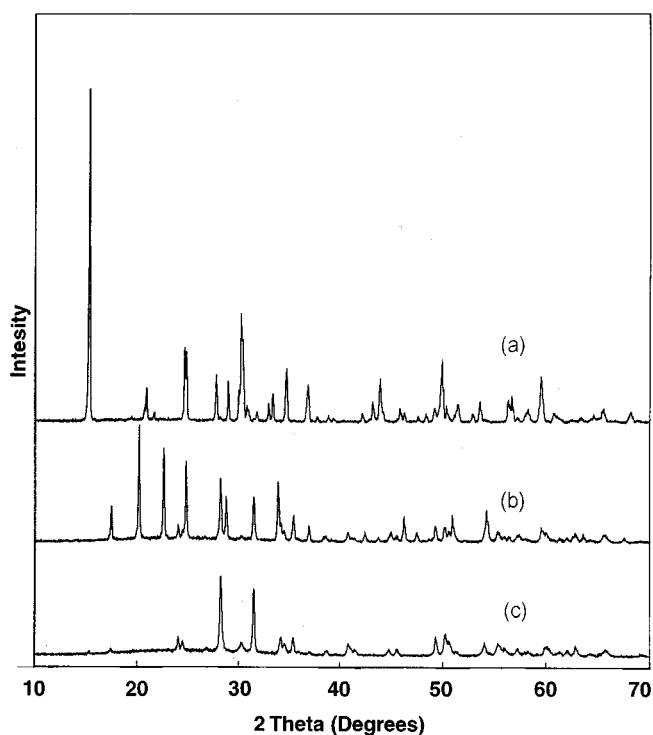


FIG. 2. X-ray powder diffraction patterns of (a) $H_xV_2Zr_2O_9 \cdot H_2O$, (b) the sample treated in air at $650^\circ C$ for 1 h, and (c) the sample treated in N_2 at $650^\circ C$ for 1 h.

amounts of V(IV) atoms. The result of EPR suggested that V and Zr atoms may appear alternatively in the framework of the product. Element analysis indicate that the components of the product are V, Zr, and the mole ratio V:Zr:O equals 1:1:5. It is expected that the small fraction of V(IV) atoms existed in the product needs equivalent amounts of protons to compensate the framework negative charges.

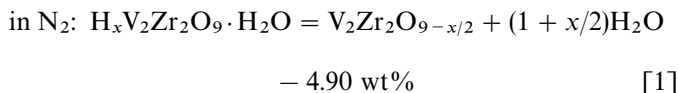
The dehydration procedure of the $H_xV_2Zr_2O_9 \cdot H_2O$ in air is different from that in N_2 due to the V(IV) oxidation only in air condition. Figures 3 and 4 show TG curves of $H_xV_2Zr_2O_9 \cdot H_2O$ in air and N_2 , respectively. A total weight loss of 4.62% over the interval from 435 to $630^\circ C$ in air was found. We can clearly see two steps of weight loss in this temperature range. A very small weight loss happened from 435 to $530^\circ C$ and a large weight loss happened from 530 to $630^\circ C$. The TG curve in N_2 shows the weight loss of 4.90% in the temperature range from 498 to $630^\circ C$. In the DTA curve of $H_xV_2Zr_2O_9 \cdot H_2O$ in N_2 , there are a significant small endothermic peak at $530^\circ C$ and a large one at $576^\circ C$, whereas in air, there was only one endothermic peak at $560^\circ C$. Weight losses in the temperature range 500 – $600^\circ C$ were attributed to dehydration of the product followed by a structural transformation. From the complex dehydrated behavior of the product in N_2 , it can be seen that there were at least two sorts of dehydration processes. One dehydration process is associated with removing one oxygen from

TABLE 1
Powder X-Ray Diffraction Data for $H_xV_2Zr_2O_9 \cdot H_2O$

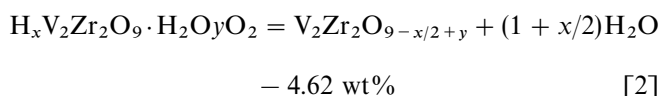
H	K	L	D_{OBS}	D_{CAL}	H	K	L	D_{OBS}	D_{CAL}
0	2	0	5.788	5.784	1	2	-3	1.989	1.991
1	0	1	4.609	4.613	2	3	2	1.978	1.979
1	1	1	4.285	4.285	4	3	0	1.961	1.962
2	1	0	4.245	4.242	3	1	2	1.913	1.914
1	2	-1	4.105	4.100	1	1	3	1.882	1.883
1	2	1	3.606	3.606	0	5	2	1.852	1.851
2	2	0	3.581	3.581	2	5	-2	1.810	1.810
1	3	-1	3.213	3.213	5	2	-1	1.786	1.786
1	0	-2	3.169	3.167	2	6	0	1.775	1.776
0	0	2	3.085	3.085	3	3	-3	1.730	1.731
0	1	2	2.980	2.981	1	4	-3	1.709	1.710
1	3	1	2.957	2.958	3	5	-2	1.695	1.695
3	1	0	2.940	2.940	2	5	2	1.632	1.633
2	0	-2	2.904	2.906	4	5	0	1.622	1.624
0	4	0	2.888	2.892	3	4	-3	1.610	1.610
2	1	-2	2.818	2.819	1	0	-4	1.586	1.586
0	2	2	2.721	2.722	5	2	1	1.579	1.580
3	2	-1	2.689	2.689	4	5	-2	1.552	1.553
1	4	-1	2.589	2.589	2	2	-4	1.527	1.527
1	3	-2	2.447	2.447	3	1	3	1.523	1.524
3	1	1	2.439	2.439	5	2	-3	1.514	1.514
3	3	-1	2.385	2.386	0	8	0	1.447	1.446
2	3	-2	2.319	2.321	4	1	-4	1.442	1.442
3	2	1	2.290	2.291	5	5	0	1.432	1.432
2	2	2	2.141	2.142	1	6	-3	1.427	1.427
3	3	-2	2.093	2.092	5	0	2	1.424	1.425
2	5	0	2.062	2.063	5	4	-3	1.379	1.379
2	4	-2	2.048	2.050	3	7	-2	1.376	1.377

structure and producing a vacancy of oxygen. In air, the oxidation of V(IV) accompanied the dehydration; the sample regained oxygen and the vacancy of oxygen was partially occupied again. This is the reason why there are different weight losses observed in air and N_2 . Another dehydration process results in the loss of one oxygen from the sample too, but does not produce vacancy of oxygen. In this process, the sites of two oxygen atoms are replaced by one oxygen atom and the structure of the sample is changed, as indicated in XRD patterns of the samples treated at temperature of $650^\circ C$ in either in air or in N_2 .

The phenomena of different weight loss in different flowing gases can be explained as follows:



in air:



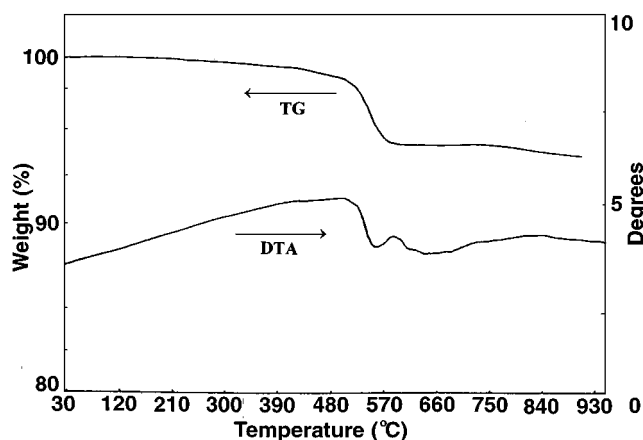


FIG. 3. TG and DTA curves of $H_xV_2Zr_2O_9 \cdot H_2O$ in air.

The value of x can be calculated from Eq. [1] to be 0.43, and we can also deduce from Eq. [2] that the vanadium (IV) can be oxidized almost completely in air, which is confirmed by EPR analysis (see Fig. 1b).

Figure 5 shows the morphology of $H_xV_2Zr_2O_9 \cdot H_2O$. All products are pure and in high crystallinity and the same shape particles as spindles with average size $30 \mu m$ were observed. We also found that the product is acidic. This was demonstrated by the fact that when the product was equilibrated with water for minutes, a weakly acidic solution was produced. For instance, when a 0.13 g sample was put into 25 ml water, the pH of the solution decreased from 6.02 to 4.80, without measurable sample dissolution.

CONCLUSIONS

In this work, a novel crystalline complex oxide, $H_xV_2Zr_2O_9 \cdot H_2O$, with vanadium(IV, V) mixed-valence,

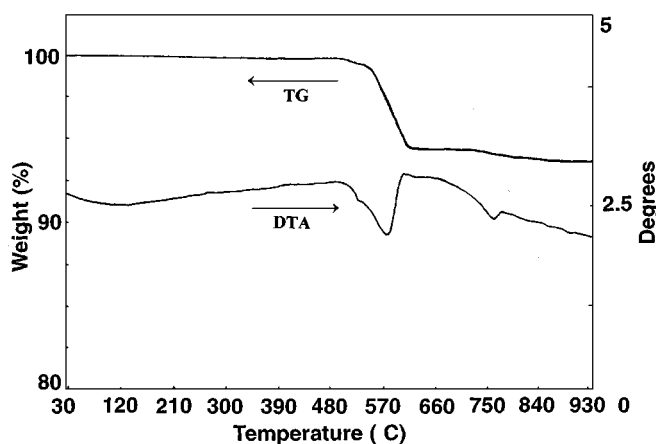


FIG. 4. TG and DTA curves of $H_xV_2Zr_2O_9 \cdot H_2O$ in N_2 .

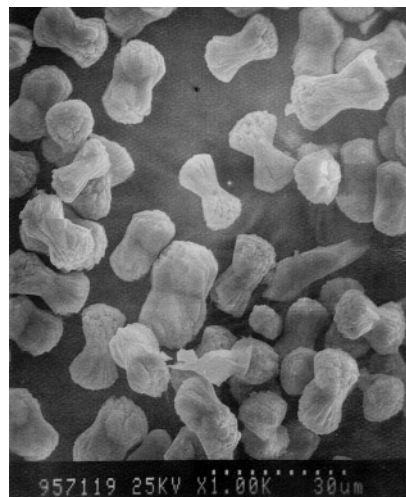


FIG. 5. Scanning electron micrograph of $H_xV_2Zr_2O_9 \cdot H_2O$.

was hydrothermally prepared. $NaVO_3$ and NH_4VO_3 can be used as vanadium sources and NaF as mineralizer. $H_xV_2Zr_2O_9 \cdot H_2O$ has monoclinic symmetry with cell parameters $a = 0.940(4) \text{ nm}$, $b = 1.156(8) \text{ nm}$, $c = 0.636(3) \text{ nm}$, $\beta = 104.1(7)^\circ$, and undergoes phase transformations at approximately $550^\circ C$ both in air and in N_2 due to the loss of water molecules and valence change of vanadium atoms in lattice. The as-made compound surface is acidic, which implies its potential application as an acidic catalyst.

ACKNOWLEDGMENTS

This work was supported by the NSFC through a National Outstanding Youth Science Fund, by the State Education Commission through an Excellent Talent Plan, and by the State Science and Technology Commission through a Pan-Deng Plan (S.F.).

REFERENCES

1. G. Centi, F. Trifiro, J. R. Ebner, and V. M. Franchetti, *Chem. Rev.* **88**, 55 (1988).
2. E. Bordes and P. Courtine, *J. Catal.* **57**, 236 (1979).
3. M. A. Chaar, D. Patel, M. C. Kung, and H. H. Kung, *J. Catal.* **105**, 483 (1987).
4. G. Centi, *Catal. Today* **16**, 5 (1993).
5. J. W. Johnson, D. C. Johnston, H. E. King, Jr., T. R. Halbert, J. F. Brody, and D. P. Goshorn, *Inorg. Chem.* **27**, 1646 (1988).
6. M. T. Pope and A. Muller, *Angew. Chem. Int. Ed. Engl.* **30**, 34 (1991).
7. L. Benhamada, A. Grandin, M. M. Borel, A. Leclaire, and B. Raveau, *J. Solid State Chem.* **104**, 193 (1993).
8. A. Grandin, J. Chardon, M. M. Borel, A. Leclaire, and B. Raveau, *J. Solid State Chem.* **104**, 226 (1993).
9. R. C. Haushalter, Q. Chen, V. Soghomonian, J. Zubieta, and C. J. O'Connor, *J. Solid State Chem.* **108**, 128 (1994).
10. R. C. Haushalter, Z. Wang, M. E. Thompson, J. Zubieta, and C. J. O'Connor, *J. Solid State Chem.* **109**, 259 (1994).
11. R. C. Haushalter, V. Soghomonian, Q. Chen, and J. Zubieta, *J. Solid State Chem.* **105**, 512 (1993).

12. R. C. Haushalter, Z. Wang, M. E. Thompson, and J. Zubieta, *Inorg. Chem.* **32**, 3700 (1990).
13. R. C. Haushalter, Z. Wang, M. E. Thompson, J. Zubieta, and C. J. O'Connoir, *Inorg. Chem.* **32**, 3966 (1993).
14. K. H. Lii, N. W. Wen, C. C. Su, and B. R. Chueh, *Inorg. Chem.* **31**, 439 (1992).
15. K. H. Lii, C. H. Li, C. Y. Cheng, and S. L. Wang, *J. Solid State Chem.* **95**, 352 (1991).
16. K. H. Lii and L. F. Mao, *J. Solid State Chem.* **96**, 436 (1992).
17. J. T. Vaughey, William T. A. Harrison, and A. J. Jacobson, *J. Solid State Chem.* **110**, 305 (1994).
18. S. Feng and M. Greenblatt, *Chem. Mater.* **4**, 462 (1992).
19. G. Li, S. Feng, and L. Li, *J. Solid State Chem.* **126**, 74 (1996).
20. C. Zhao, S. Feng, Z. Chao, C. Shi, R. Xu, and J. Ni, *J. Chem. Soc. Chem. Commun.*, 1641 (1996).
21. A. Boulouf and D. Louer, *J. Appl. Crystallogr.* **24**, 987 (1991).
22. G. S. Smith and R. L. Snyder, *J. Appl. Crystallogr.* **12**, 60 (1979).